Supporting Information

Synthesis of Cu@ZnO_{1-x}/Al_2O_3 catalyst with high-density ZnO_{1-x}-Cu interfacial sites for enhanced CO_2 hydrogenation to methanol

Yunshuo Wu[1,2,3], Haiqiang Wang[1,2,3]*, Zhongbiao Wu[1,2,3]*

[1] College of Environmental & Resource Sciences, Zhejiang University, Hangzhou 310058, P.R. China.
[2] Key Laboratory of Environment Remediation and Ecological Health, Ministry of Education, Zhejiang University, Hangzhou 310058, P.R. China.
[3] Zhejiang Provincial Engineering Research Center of Industrial Boiler Furnace Flue Gas Pollution Control, Hangzhou 310058, P.R. China.

*Corresponding author. Email: haiqiangwang@zju.edu.cn (H.W.); zbwu@zju.edu.cn (Z.W.)

This PDF file includes:

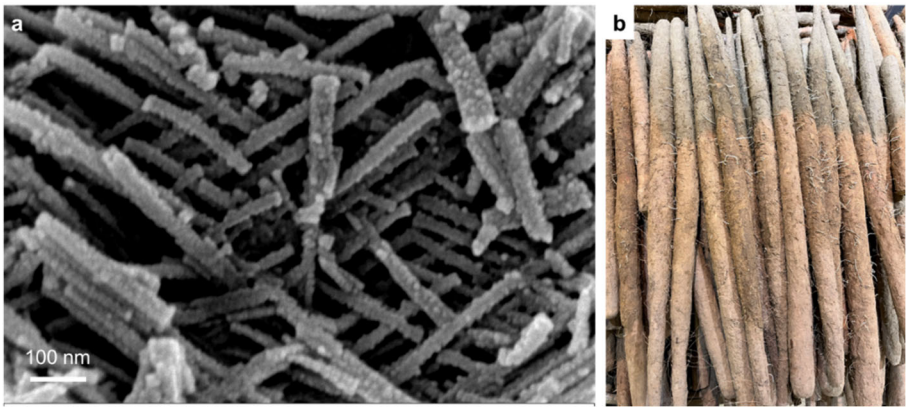

Figure S1. (a) FE-SEM image of fresh $Cu@ZnO_{1-x}/Al_2O_3$. (b) A photo of Chinese-yam.

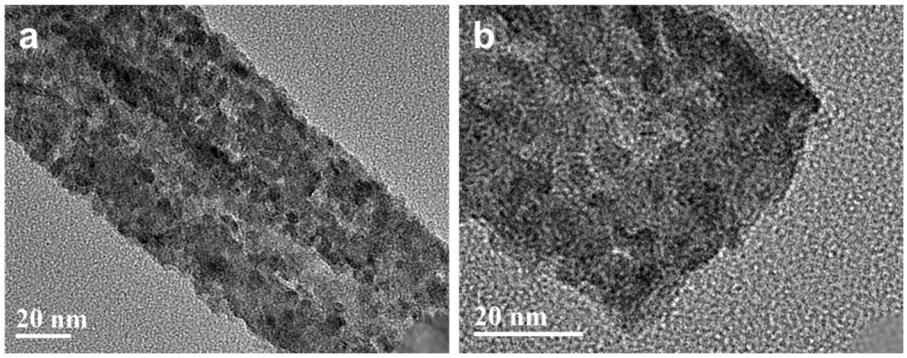

Figure S2. HR-TEM image of fresh $Cu@ZnO_{1-x}/Al_2O_3$ before H_2 reduction.

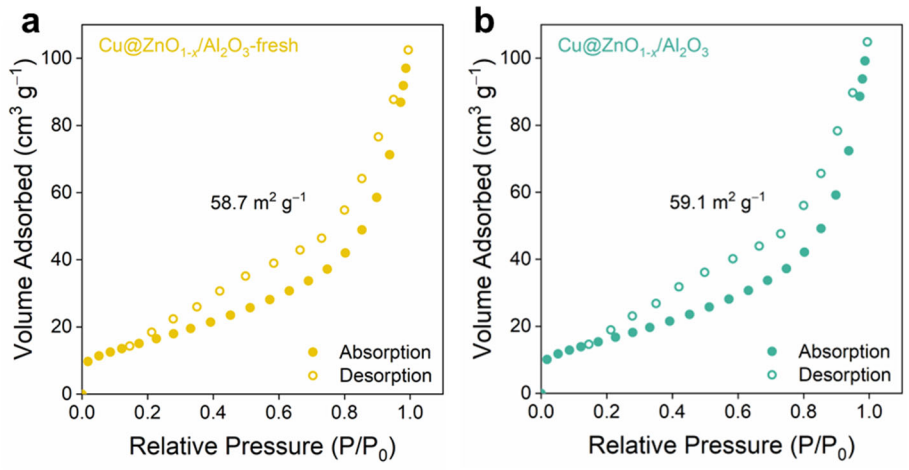

Figure S3. N_2 sorption experiments of (a) fresh and (b) reduced $Cu@ZnO_{1-x}/Al_2O_3$.

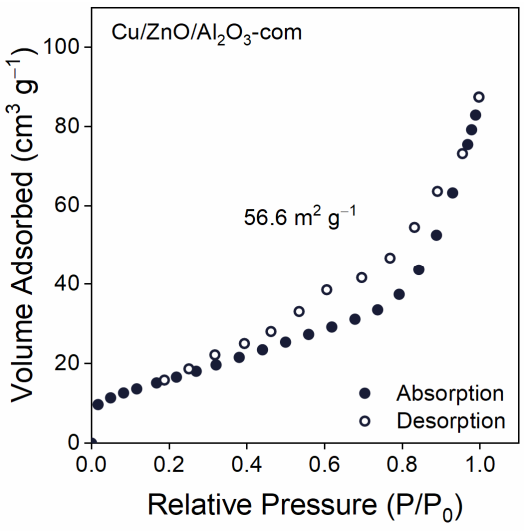

Figure S4. N_2 sorption experiments of reduced Cu/ZnO/Al_2O_3-com.

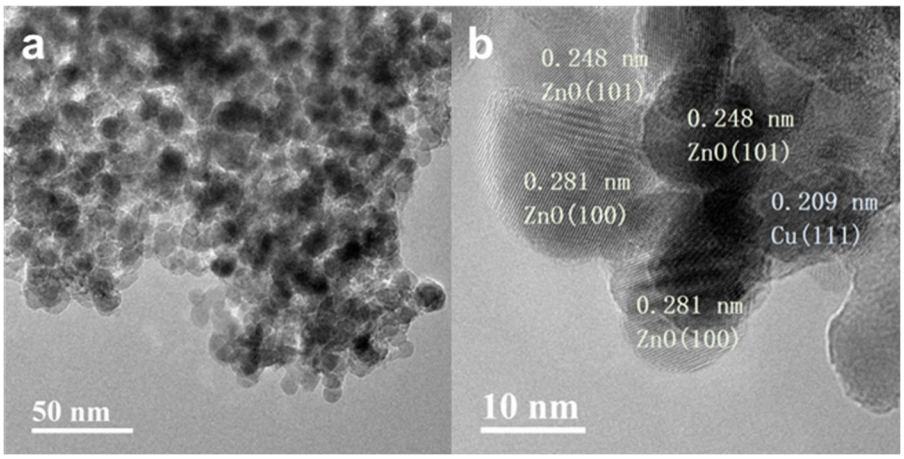

Figure S5. (a) TEM and (b) HR-TEM images of CuZnAl-170-170.

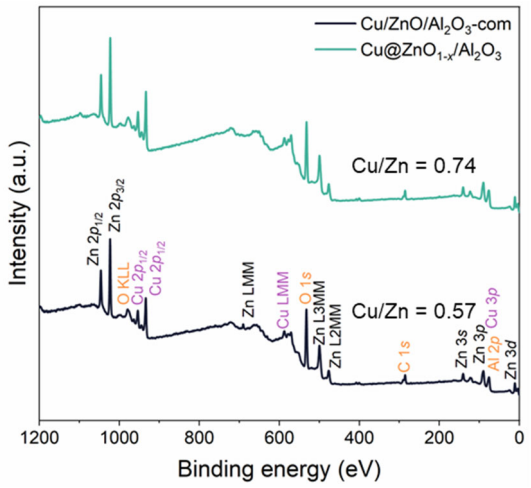

Figure S6. XPS survey spectra of Cu/ZnO/Al_2O_3-com and Cu@ZnO_{1-x}/Al_2O_3.

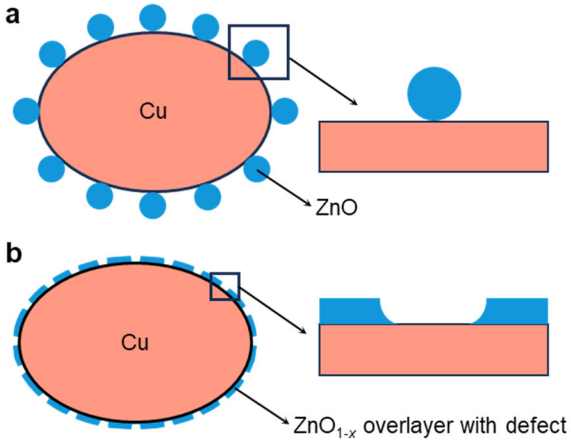

Figure S7. (a−b) Schematic diagram of Cu/ZnO/Al_2O_3-com (a) and Cu@ZnO1-*x*/Al_2O_3 (b).

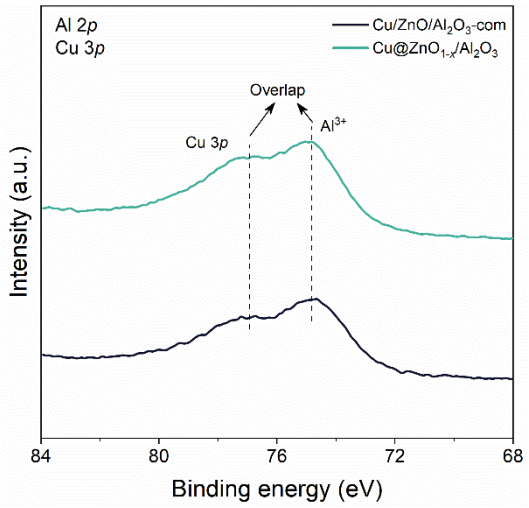

Figure S8. XPS overlaps between Al 2*p* and Cu 3*p* of Cu/ZnO/Al_2O_3-com and Cu@ZnO_{1-x}/Al_2O_3.

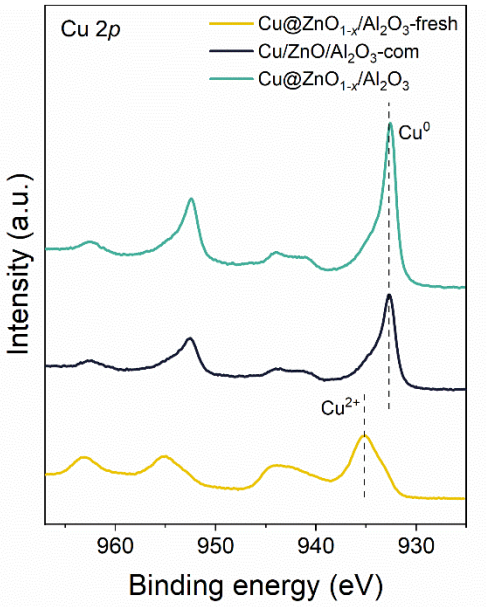

Figure S9. Cu 2*p* XPS spectra of Cu@ZnO_{1-x}/Al_2O_3-fresh, Cu@ZnO_{1-x}/Al_2O_3, and Cu/ZnO/Al_2O_3-com.

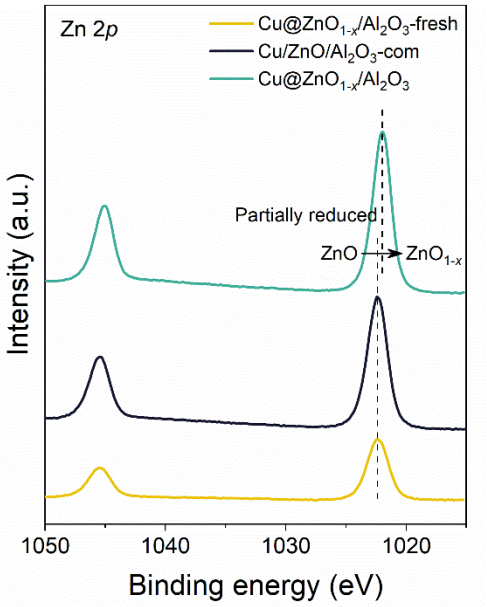

Figure S10. Zn 2*p* XPS spectra of Cu@ZnO_{1-x}/Al_2O_3-fresh, Cu@ZnO_{1-x}/Al_2O_3, and Cu/ZnO/Al_2O_3-com.

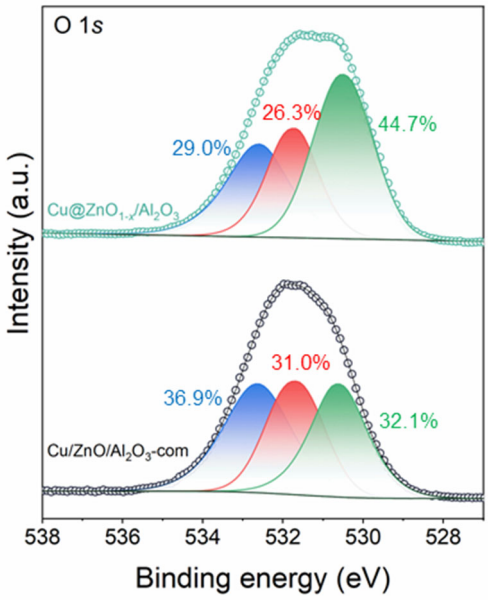

Figure S11. O 1*s* XPS spectra of $Cu@ZnO_{1-x}/Al_2O_3$ and $Cu/ZnO/Al_2O_3$-com.

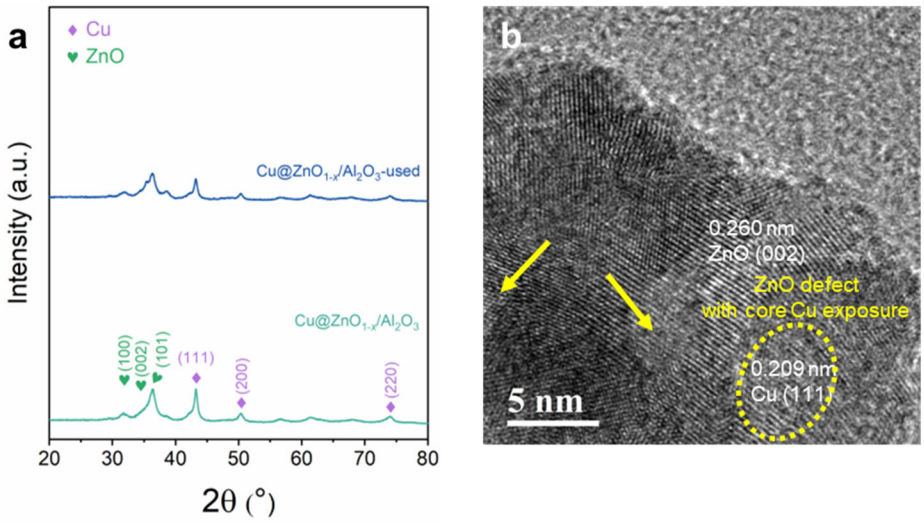

Figure S12. (a) XRD patterns, and (b) TEM images of $Cu@ZnO_{1-x}/Al_2O_3$-used.

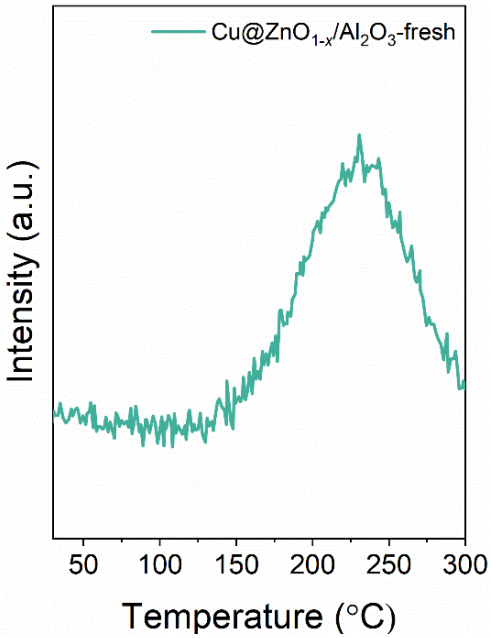

Figure S13. H_2 consumption profile at different temperatures in 5% H_2/Ar for the Cu@ZnO_{1-x}/Al_2O_3-fresh.

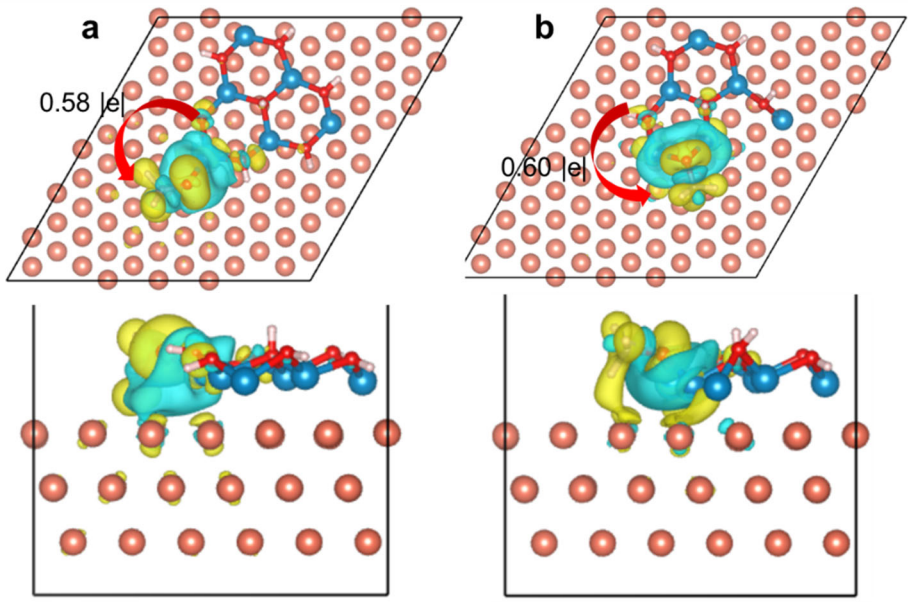

Figure S14. (a–b) Charge density differences ($\delta\rho = \rho_{A+B} - \rho_A - \rho_B$) of CH_3O^* species adsorbed on Zn_6O/Cu(111) interface (a), and Zn_6O_{1-x}/Cu(111) interface (b). Yellow and cyan colors respectively represent e^- accumulation and depletion.

Table S1. Metal contents obtained by ICP-OES.

Sample	**Cu/ZnO/Al_2O_3-com**	**Cu@ZnO_{1-x}/Al_2O_3**
Cu (wt.%)	52.6	51.4
Zn (wt.%)	25.5	25.4
Al (wt.%)	4.3	4.5
O (wt.%)[a]	17.6	18.7

[a] The O content was not directly determined by ICP-OES, but calculated since the catalysts only consisted of these four elements (The Na residue was considered negligible due to its extremely low content, which was less than 0.1 wt.%).

Table S2. Catalytic performance in CO_2 hydrogenation over various reported catalysts.

Catalysts	P/MPa	T/°C	GHSV	H_2/CO_2	Con.[a]	Sel.[b]	STY[c]	Ref.	Year
$CuZnGa/SiO_2$	2	270	18000	3	5.6	99.5	348.8	[1]	2001
CuZnMn	5	250	12000	3	22.3	43.0	420	[2]	2013
CuZnAl	5	250	12000	3	13.4	58.1	300	[3]	2015
CuZnAlY	5	250	12000	3	20.2	69.3	520	[3]	2015
In_2O_3	4	330	15000	3	7.1	39.7	118.1	[4]	2015
Cu/SiO_2	3	320	16000	4	28	21.3	260	[5]	2015
Pd/ZnO	2	250	3600	3	10.7	60	77.4	[6]	2016
In_2O_3/ZrO_2	5	300	20000	4	5.2	99.8	321	[7]	2016
$Cu_1La_{0.2}$/SBA-15	3	240	12000	3	6	81.2	200.7	[8]	2019
In_2O_3@ZIF-67(Co)	5	270	17200	4	12.5	83	510	[9]	2020
Co@S1	3	240	6000	3	15.2	47.6	141.8	[10]	2020
S_v-MoS_2	5	180	3000	3	12.5	94.3	115.5	[11]	2021
Si-Cu-ZnO	3	280	18000	3	8.3	19	97.4	[12]	2022
Ce-CuZn-MOF	2.8	260	20000	3	8.0	71.1	400.3	[13]	2024
$Cu@ZnO_{1-x}/Al_2O_3$	3	240	12000	3	19.4	63	454.6	[d]	

[a] CO_2 conversion (%). [b] Selectivity of methanol (%). [c] Space time yield of methanol ($g \cdot kg_{cat}^{-1} \cdot h^{-1}$). [d] This work.

Table S3. Summarized Raman shifts of likely compounds.

Compounds	**Raman shift (cm^{-1})**	**References**
Hydrogen bonded OH of the brucite-like layers	200−300	[14]
CuO	293 (A_g)	[14]
CuO	341 and 630 (B_g)	[15], [16]
Chemisorbed CO on copper surface	282	[17]
Chemisorbed CO_2 on copper surface	529	[18]
Chemisorbed H_2O on copper surface	~624 (broad)	[19]
Cu–CO stretching	355–366	[17]
C-containing species binding to the Cu surface	486−500 526−536	[20]
ZnO	101 and 437 (E_2) 381 (transverse A_1) 407 (transverse E_1) 574 (longitudinal A_1) 583 (longitudinal E_1)	[21]
ZnO with lattice defect	580 (E_1(LO))	[22]
Symmetric CO_3 stretching vibration	1106 (v_1)	[23]
Symmetric CO stretching vibration	980−1050	[24]
Carbonate group	837 (v_2)	[25], [26]
Relative translations between the cation and carbonate groups	176	[23]
Carbon materials	1350 (D) 1580 (G)	[27]
Metallic copper	/	[28]

Table S4. Potential energy values (eV) in **Fig. 8**.

Steps	**Zn_6O/Cu(111)**	**$Zn_{10}O$/Cu(111)**	**Zn_6O_{1-x}/Cu(111)**	**$Zn_{10}O_{1-x}$/Cu(111)**
$CO_2(g)+3H_2(g)$	0.000	0.000	0.000	0.000
$CO_2*+3H_2(g)$	−0.305	−0.234	−0.318	−0.320
$CO_2*+H*+5/2H_2(g)$	−0.625	−0.582	−0.623	−0.639
TS1	−0.021	0.173	−0.117	0.025
$HCOO*+5/2H_2(g)$	−0.818	−0.939	−1.270	−1.255
$HCOO*+H*+2H_2(g)$	−1.181	−1.421	−1.644	−1.891
TS2	−0.231	−0.573	−1.090	−1.221
$HCOOH*+2H_2(g)$	−0.938	−1.076	−1.239	−1.322
$HCOOH*+H*+3/2H_2(g)$	−1.316	−1.351	−1.433	−1.507
TS3	−0.500	−0.630	−0.634	−0.666
$H_2COOH*+3/2H_2(g)$	−0.866	−1.003	−1.048	−1.190
TS4	−0.155	−0.060	−0.310	−0.367
$CH_2O*+OH*+3/2H_2(g)$	−0.706	−0.504	−0.860	−0.817
$CH_2O*+OH*+H*+H_2(g)$	−0.944	−0.754	−1.214	−1.081
TS5	−0.289	−0.485	−0.467	−0.386
$CH_2O*+H_2O*+H_2(g)$	−1.076	−1.224	−1.300	−1.464
$CH_2O*+H_2O(g)+H_2(g)$	−0.564	−0.674	−0.802	−0.814
$CH_2O*+H*+H_2O(g)+1/2H_2(g)$	−0.912	−0.956	−1.118	−1.110
TS6	−0.721	−0.838	−0.885	−0.755
$CH_3O*+H_2O(g)+1/2H_2(g)$	−1.081	−1.316	−2.450	−2.583
$CH_3O*+H*+H_2O(g)$	−1.547	−1.662	−2.711	−2.857
TS7	−1.245	−1.479	−1.937	−1.988
$CH_3OH*+H_2O(g)$	−2.175	−2.284	−2.104	−2.226
$CH_3OH(g)+H_2O(g)$	−1.194	−1.194	−1.194	−1.194

SI References

(1) Toyir, J.; de la Piscina, P. R. r.; Fierro, J. L. G.; Homs, N. s. Highly effective conversion of CO_2 to methanol over supported and promoted copper-based catalysts: influence of support and promoter. *Appl. Catal. B* **2001**, *29* (3), 207-215.
(2) Gao, P.; Li, F.; Zhao, N.; Xiao, F.; Wei, W.; Zhong, L.; Sun, Y. Influence of modifier (Mn, La, Ce, Zr and Y) on the performance of Cu/Zn/Al catalysts via hydrotalcite-like precursors for CO_2 hydrogenation to methanol. *Appl. Catal. A* **2013**, *468*, 442-452.
(3) Gao, P.; Zhong, L.; Zhang, L.; Wang, H.; Zhao, N.; Wei, W.; Sun, Y. Yttrium oxide modified Cu/ZnO/Al_2O_3 catalysts via hydrotalcite-like precursors for CO_2 hydrogenation to methanol. *Catal. Sci. Technol.* **2015**, *5* (9), 4365-4377.
(4) Sun, K.; Fan, Z.; Ye, J.; Yan, J.; Ge, Q.; Li, Y.; He, W.; Yang, W.; Liu, C.-j. Hydrogenation of CO_2 to methanol over In_2O_3 catalyst. *J. CO_2 Util.* **2015**, *12*, 1-6.
(5) Wang, Z.-Q.; Xu, Z.-N.; Peng, S.-Y.; Zhang, M.-J.; Lu, G.; Chen, Q.-S.; Chen, Y.; Guo, G.-C. High-Performance and Long-Lived Cu/SiO_2 Nanocatalyst for CO_2 Hydrogenation. *ACS Catal.* **2015**, *5* (7), 4255-4259.
(6) Bahruji, H.; Bowker, M.; Hutchings, G.; Dimitratos, N.; Wells, P.; Gibson, E.; Jones, W.; Brookes, C.; Morgan, D.; Lalev, G. Pd/ZnO catalysts for direct CO_2 hydrogenation to methanol. *J. Catal.* **2016**, *343*, 133-146.
(7) Martin, O.; Martín, A. J.; Mondelli, C.; Mitchell, S.; Segawa, T. F.; Hauert, R.; Drouilly, C.; Curulla-Ferré, D.; Pérez-Ramírez, J. Indium Oxide as a Superior Catalyst for Methanol Synthesis by CO_2 Hydrogenation. *Angew. Chem. Int. Ed.* **2016**, *55* (21), 6261-6265.
(8) Chen, K.; Fang, H.; Wu, S.; Liu, X.; Zheng, J.; Zhou, S.; Duan, X.; Zhuang, Y.; Chi Edman Tsang, S.; Yuan, Y. CO_2 hydrogenation to methanol over Cu catalysts supported on La-modified SBA-15: The crucial role of Cu–LaO_x interfaces. *Appl. Catal. B* **2019**, *251*, 119-129.
(9) Pustovarenko, A.; Dikhtiarenko, A.; Bavykina, A.; Gevers, L.; Ramírez, A.; Russkikh, A.; Telalovic, S.; Aguilar, A.; Hazemann, J.-L.; Ould-Chikh, S.; Gascon, J. Metal–Organic Framework-Derived Synthesis of Cobalt Indium Catalysts for the Hydrogenation of CO_2 to Methanol. *ACS Catal.* **2020**, *10* (9), 5064-5076.
(10) Wang, L.; Guan, E.; Wang, Y.; Wang, L.; Gong, Z.; Cui, Y.; Meng, X.; Gates, B. C.; Xiao, F.-S. Silica accelerates the selective hydrogenation of CO_2 to methanol on cobalt catalysts. *Nat. Commun.* **2020**, *11* (1), 1033.
(11) Hu, J.; Yu, L.; Deng, J.; Wang, Y.; Cheng, K.; Ma, C.; Zhang, Q.; Wen, W.; Yu, S.; Pan, Y.; Yang, J.; Ma, H.; Qi, F.; Wang, Y.; Zheng, Y.; Chen, M.; Huang, R.; Zhang, S.; Zhao, Z.; Mao, J.; Meng, X.; Ji, Q.; Hou, G.; Han, X.; Bao, X.; Wang, Y.; Deng, D. Sulfur vacancy-rich MoS_2 as a catalyst for the hydrogenation of CO_2 to methanol. *Nat. Catal.* **2021**, *4* (3), 242-250.

(12) Shao, Y.; Kosari, M.; Xi, S.; Zeng, H. C. Single Solid Precursor-Derived Three-Dimensional Nanowire Networks of CuZn-Silicate for CO_2 Hydrogenation to Methanol. *ACS Catal.* **2022**, *12* (10), 5750-5765.
(13) Ye, R.; Ma, L.; Mao, J.; Wang, X.; Hong, X.; Gallo, A.; Ma, Y.; Luo, W.; Wang, B.; Zhang, R.; Duyar, M. S.; Jiang, Z.; Liu, J. A Ce-CuZn catalyst with abundant Cu/Zn-Ov-Ce active sites for CO_2 hydrogenation to methanol. *Nat. Commun.* **2024**, *15* (1), 2159.
(14) Álvarez-Hernández, D.; Marín-Sánchez, M.; Lobo-Andrades, L.; Azancot, L.; Bobadilla, L. F.; Ivanova, S.; Centeno, M. A. Low-temperature reverse water gas-shift reaction over highly efficient Cu-hydrotalcites: Mechanistic insights on the role of malachite phase. *Catal. Today* **2023**, *422*, 114235.
(15) Santos, J. L.; Reina, T. R.; Ivanova, S.; Centeno, M. A.; Odriozola, J. A. Gold promoted Cu/ZnO/Al_2O_3 catalysts prepared from hydrotalcite precursors: Advanced materials for the WGS reaction. *Appl. Catal. B* **2017**, *201*, 310-317.
(16) Anu, A.; Abdul Khadar, M. CuO–ZnO nanocomposite films with efficient interfacial charge transfer characteristics for optoelectronic applications. *SN Appl. Sci.* **2019**, *1* (9), 1057.
(17) Gao, J.; Zhang, H.; Guo, X.; Luo, J.; Zakeeruddin, S. M.; Ren, D.; Grätzel, M. Selective C–C Coupling in Carbon Dioxide Electroreduction via Efficient Spillover of Intermediates As Supported by Operando Raman Spectroscopy. *J. Am. Chem. Soc.* **2019**, *141* (47), 18704-18714.
(18) Zhang, Z.-Y.; Tian, H.; Bian, L.; Liu, S.-Z.; Liu, Y.; Wang, Z.-L. Cu-Zn-based alloy/oxide interfaces for enhanced electroreduction of CO_2 to C_{2+} products. *J. Energy Chem.* **2023**, *83*, 90-97.
(19) Chen, Y. X.; Zou, S. Z.; Huang, K. Q.; Tian, Z. Q. SERS studies of electrode/electrolyte interfacial water part II—librations of water correlated to hydrogen evolution reaction. *J. Raman Spectrosc.* **1998**, *29* (8), 749-756.
(20) Lei, Q.; Huang, L.; Yin, J.; Davaasuren, B.; Yuan, Y.; Dong, X.; Wu, Z.-P.; Wang, X.; Yao, K. X.; Lu, X.; Han, Y. Structural evolution and strain generation of derived-Cu catalysts during CO2 electroreduction. *Nat. Commun.* **2022**, *13* (1), 4857.
(21) Damen, T. C.; Porto, S. P. S.; Tell, B. Raman Effect in Zinc Oxide. *Phys. Rev.* **1966**, *142* (2), 570-574.
(22) Liu, X.; Luo, J.; Wang, H.; Huang, L.; Wang, S.; Li, S.; Sun, Z.; Sun, F.; Jiang, Z.; Wei, S.; Li, W.-X.; Lu, J. In Situ Spectroscopic Characterization and Theoretical Calculations Identify Partially Reduced ZnO_{1-x}/Cu Interfaces for Methanol Synthesis from CO_2. *Angew. Chem. Int. Ed.* **2022**, *61* (23), e202202330.
(23) Gunasekaran, S.; Anbalagan, G.; Pandi, S. Raman and infrared spectra of carbonates of calcite structure. *J. Raman Spectrosc.* **2006**, *37* (9), 892-899.
(24) Petersen, P.; Krasser, W. Surface enhanced Raman scattering from a ternary catalyst Cu/ZnO/Al_2O_3 under reaction conditions. *Appl. Surf. Sci.* **1996**, *103* (1), 91-100.

(25) Frost, R. L.; Martens, W. N.; Rintoul, L.; Mahmutagic, E.; Kloprogge, J. T. Raman spectroscopic study of azurite and malachite at 298 and 77 K. *J. Raman Spectrosc.* **2002**, *33* (4), 252-259.
(26) Frost, R. L.; Hales, M. C.; Jagannadha Reddy, B. Aurichalcite – An SEM and Raman spectroscopic study. *Polyhedron* **2007**, *26* (13), 3291-3300.
(27) Tuinstra, F.; Koenig, J. L. Raman spectrum of graphite. *J. Chem. Phys.* **1970**, *53* (3), 1126-1130.
(28) Raman, C. V.; Krishnan, K. S. A New Type of Secondary Radiation. *Nature* **1928**, *121* (3048), 501-502.